Calculations of the dynamic dipole polarizabilities for the Li^+ ion*

Yong-Hui Zhang(张永慧)[1,2], Li-Yan Tang(唐丽艳)[2,†], Xian-Zhou Zhang(张现周)[1], and Ting-Yun Shi(史庭云)[2]

[1] *Department of Physics, Henan Normal University, Xinxiang* 453007, *China*

[2] *State Key Laboratory of Magnetic Resonance and Atomic and Molecular Physics, Wuhan Institute of Physics and Mathematics, Chinese Academy of Sciences, Wuhan* 430071, *China*

(Received 31 March 2016; revised manuscript received 23 May 2016; published online 25 August 2016)

The B-spline configuration-interaction method is applied to the investigations of dynamic dipole polarizabilities for the four lowest triplet states (2^3S, 3^3S, 2^3P, and 3^3P) of the Li^+ ion. The accurate energies for the triplet states of n^3S, n^3P, and n^3D, the dipole oscillator strengths for $2^3S(3^3S) \rightarrow n^3P$, $2^3P(3^3P) \rightarrow n^3S$, and $2^3P(3^3P) \rightarrow n^3D$ transitions, with the main quantum number n up to 10 are tabulated for references. The dynamic dipole polarizabilities for the four triplet states under a wide range of photon energy are also listed, which provide input data for analyzing the Stark shift of the Li^+ ion. Furthermore, the tune-out wavelengths in the range from 100 nm to 1.2 μm for the four triplet states, and the magic wavelengths in the range from 100 nm to 600 nm for the $2^3S \rightarrow 3^3S$, $2^3S \rightarrow 2^3P$, and $2^3S \rightarrow 3^3P$ transitions are determined accurately for the experimental design of the Li^+ ion.

Keywords: triplet states of Li^+ ion, dynamic dipole polarizabilities, tune-out wavelength, magic wavelength

PACS: 31.15.ac, 31.15.ap, 32.10.Dk **DOI:** 10.1088/1674-1056/25/10/103101

1. Introduction

Since the relativistic and QED corrections in the Li^+ ion should be larger than in helium due to the Z^4 scaling of the energy, the studies of the Li^+ ion are of great interest because of its wide applications. For example, the combination between the experimental measurements and the theoretical calculations of the 2^3S hyperfine splitting for the Li^+ ion provides a sensitive test of the hyperfine atomic structure theory,[1–3] and the investigation of the 2^3P_J fine structure of the Li^+ ion can be used to determine the fine structure constant.[4–8] In addition, the high-precision measurement of the $2^3S \rightarrow 2^3P$ transition for the Li^+ ion isotopes could be used to test the relativistic and QED corrections,[2,3,9] to extract the relative nuclear charge radius,[10] to test the time dilation and verify the special relativity.[11]

The dynamic dipole polarizabilities of ions, which describe the distortion of the electronic charge distribution in the presence of an oscillating electric field with angular frequency ω, play an important role in the calculations of the van der Waals C_6 coefficient,[12,13] in the determinations of refractive index and dielectric constants of ionic crystals,[14] in the construction of a core-polarization model for atoms and molecules,[15,16] and in the analysis of the Stark shifts.[17–19] Especially, the tune-out and magic wavelengths,[18,20,21] which are extracted from the dynamic dipole polarizabilities, become important parameters for experimental design of ion trapping. For example, recently, Liu *et al.* suggested that the magic wavelengths of ions pave a way to build an all-optical trapped ion[17,22–24] to eliminate the second-order of Ac Stark shift.

At present, there many works reporting the calculation of the static dipole polarizability of the ground-state Li^+ ion.[25–31] For example, Zhu *et al.* computed the nonrelativisitc polarizabilities by using Hylleraas basis,[29] Johnson and Cheng got the polarizability by exploiting the B-spline relativistic configuration interaction (CI) method to solve the Dirac–Coulomb–Breit equation,[30] and Lim *et al.* obtained the polarizability by using the fully relativistic coupled-cluster method.[32] For the dynamic polarizabilities of the Li^+ ion, Chung applied the variational perturbation method into the calculation of the ground state dynamic dipole polarizabilities,[33] and Glover and Weinhold obtained the rigorous upper and lower bounds for dynamic dipole polarizabilities with the laser frequency up to the first excitation threshold of the ground state.[25] However, compared with the ground-state polarizabilities, there are several calculations of polarizabilities for the triplet states of the Li^+ ion. For example, the static dipole polarizability for the 2^3S and 2^3P states can be found in Refs. [34]–[36], only two works[37,38] about the dynamic polarizabilities for the 2^3S state were published, and there has been no work reported for the dynamic dipole polarizabilities of other triplet states of the Li^+ ion in the literature.

In the present study, the CI method based on B-spline functions developed in our previous work[39] is extended to calculate the dynamic dipole polarizabilities for the four lowest triplet states of the Li^+ ion. The tune-out wavelengths for the 2^3S, 2^3P, 3^3S, and 3^3P states are determined, and the magic wavelengths for the $2^3S \rightarrow 3^3S$, $2^3S \rightarrow 2^3P$, and

*Project supported by the National Basic Research Program of China (Grant No. 2012CB821305) and the National Natural Science Foundation of China (Grant Nos. 11474319, 11274348, and 91536102).

†Corresponding author. E-mail: lytang@wipm.ac.cn

© 2016 Chinese Physical Society and IOP Publishing Ltd

$2^3S \rightarrow 3^3P$ transitions are tabulated for reference. Atomic units are used throughout this paper unless specifically mentioned.

2. Structure calculations

2.1. B-spline CI method

Taking the Li^+ ion as a Coulomb three-body system, choosing the atomic nucleus as particle 0 and two electrons as particle 1 and particle 2, respectively, the Hamiltonian can be written as

$$H = -\sum_{i=1}^{2}\frac{\nabla_i^2}{2} - \sum_{i=1}^{2}\frac{3}{r_i} + \frac{1}{r_{12}}, \quad (1)$$

where $r_{12} = |\boldsymbol{r}_1 - \boldsymbol{r}_2|$ is the distance between two electrons.

Recently, significant progress has been made in the variational calculations for two-electron systems by using the B-spline CI basis set,[39–42] which has the following functional form,

$$\begin{aligned}\phi_{ij}(LS) = \eta_{ij}\sum_{m_i m_j}\sum_{m_{s_i} m_{s_j}} &\langle \ell_i m_i; \ell_j m_j | LM\rangle \langle 1/2 m_{s_i}; 1/2 m_{s_j} | SM_S\rangle \\ &\times \frac{1}{\sqrt{2}}\big[R_i(r_1) Y_{\ell_i m_i}(\hat{r}_1)\chi_i(1) R_j(r_2) Y_{\ell_j m_j}(\hat{r}_2)\chi_j(2) \\ &- R_j(r_1) Y_{\ell_j m_j}(\hat{r}_1)\chi_j(1) R_i(r_2) Y_{\ell_i m_i}(\hat{r}_2)\chi_i(2)\big], \quad (2)\end{aligned}$$

where η_{ij} is a normalization constant, the Clebsch–Gordan coefficients $\langle \ell_i m_i; \ell_j m_j | LM\rangle$ and $\langle 1/2 m_{s_i}; 1/2 m_{s_j} | SM_S\rangle$ represent ℓ–ℓ and s–s coupling, and $R_i(r) Y_{\ell_i m_i}(\hat{r})\chi_i$ is the i-th eigen-wavefunction of the single-electron Schrödinger equation with eigen-energy of ε_i. The radial wavefunction $R_i(r)$ is expanded as the B-spline functions,[39]

$$R_i(r) = \sum_j c_j^i B_j(r). \quad (3)$$

Using the variational method, the expectation value of the Hamiltonian can be simplified to the following configuration equation,

$$\sum_{k\ell}\big[(\varepsilon_i + \varepsilon_j)\delta_{ik}\delta_{jl} + V_{ijkl}\big]c_{kl} = \lambda c_{ij}, \quad (4)$$

where λ and c_{ij} are respectively the eigen-energies and the expansion coefficients of eigen-wavefunction for the Li^+ ion, the expression of the potential-energy matrix element $V_{ijk\ell}$ can be found in our previous paper about helium.[39]

The present CI calculation is performed by fixing the box size $R_0 = 150$ a.u. (the unit a.u. is short for atomic unit), the nonlinear parameter $\gamma = R_0 \times 0.042$, and the order of the B-spline $k = 7$. The convergence test of the energies and oscillator strengths are performed as the number of B-spline N and partial waves ℓ_{max} increased. The maximum N and ℓ_{max} used in our calculation are respectively 40 and 10.

2.2. Energies and oscillator strengths

Figure 1 is a diagram about the nonrelativistic triplet energy levels of the Li^+ ion, where some important transitions are labeled with arrows. Compared with our previous work of Ref. [39], the energies and oscillator strengths have similar convergent styles to helium.[39]

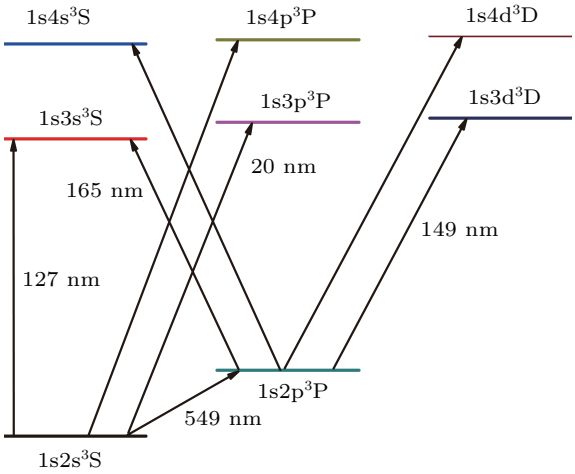


Fig. 1. (color online) Low-lying triplet energy levels of the Li^+ ion.

Table 1. Comparison of the energies (in unit a.u.) for the Li^+ ion. The experimental data were taken from the National Institute of Science and Technology (NIST) tabulation.[43] The numbers in the parentheses are the computational uncertainties.

State	Present	Experiment[43]	Ref. [44]
2^3S	−5.1107273(1)	−5.11074769	−5.110727372509
3^3S	−4.7520764(2)	−4.75207504	−4.752076455858
4^3S	−4.6371366(2)	−4.63713292	−4.637136594629
5^3S	−4.5860927(2)	−4.58608861	−4.586092669796
6^3S	−4.5590386(2)	−4.55903451	−4.559038618569
7^3S	−4.542992(2)	−4.54298732	
8^3S	−4.532699(2)	−4.53269420	
9^3S	−4.525704(2)		
10^3S	−4.520735(3)		
2^3P	−5.0277156(1)	−5.02770270	−5.0277156770
3^3P	−4.7304597(2)	−4.73045113	−4.7304596641
4^3P	−4.6284636(2)	−4.62845652	−4.6284635563
5^3P	−4.5817684(2)	−4.58176287	−4.5817684035
6^3P	−4.5565768(2)	−4.55657226	−4.5565767839
7^3P	−4.541458(2)		
8^3P	−4.531680(2)		
9^3P	−4.524993(2)		
10^3P	−4.520219(3)		
3^3D	−4.7225269(1)	−4.72251035	−4.7225269124
4^3D	−4.6251508(2)	−4.62514206	−4.6251507732
5^3D	−4.5800824(2)	−4.58007680	−4.5800824257
6^3D	−4.5556049(2)	−4.55560085	−4.5556048684
7^3D	−4.540848(1)	−4.54084511	
8^3D	−4.531272(2)	−4.53126879	
9^3D	−4.524707(2)		
10^3D	−4.520010(3)		

Table 1 lists final extrapolated energies for n^3S, n^3P, and n^3D states of the Li^+ ion with the main quantum number of

n up to 10. It is clearly seen that all the energies have at least six significant digits and can compare well with the experimental values from NIST.[43] Especially for the 2^3S and 2^3P states, the energies are respectively $-5.1107273(1)$ a.u. and $-5.0277156(1)$ a.u., which are in excellent agreement with the Hylleraas values of Cann *et al.*[44] and much more accurate than the results of Refs. [45] and [46]. For the 3^3S and 3^3P states, present values of $-4.7520764(2)$ a.u. and $-4.7304597(2)$ a.u. have seven significant digits compared with the values of Ref. [44].

The extrapolated oscillator strengths for some selective dipole transitions are presented in Table 2, and comparisons with other published values are also listed in this table. All of our results are in good agreement with the explicitly correlated wavefunction calculations of Ref. [44]. For the $2^3\mathrm{S} \rightarrow 2^3\mathrm{P}$ transition, our result of 0.3079405(3) is in perfect agreement with the value of 0.3079402 in Ref. [47] and more accurate than the value of 0.307944 by two orders of magnitude.[44] For the $2^3\mathrm{P} \rightarrow 3^3\mathrm{D}$ transition, the present result agrees well with the values of Refs. [47] and [48]. Even for the dipole transitions involved in the unnatural-parity states, both the oscillator strengths of $2^3\mathrm{P} \rightarrow 2^3\mathrm{P}^\mathrm{e}$ and $3^3\mathrm{P} \rightarrow 3^3\mathrm{P}^\mathrm{e}$ transitions have four significant digits.

Table 2. Comparison of the oscillator strengths for the Li^+ ion. The numbers in the parentheses represent computational uncertainties.

Transition	Present	Ref. [44]	Transition	Present	Ref. [44]
$2^3\mathrm{S} \rightarrow 2^3\mathrm{P}$	0.307941(1)	0.307944	$3^3\mathrm{S} \rightarrow 2^3\mathrm{P}$	0.117097(1)	0.11709
$2^3\mathrm{S} \rightarrow 3^3\mathrm{P}$	0.187054(1)	0.18707	$3^3\mathrm{S} \rightarrow 3^3\mathrm{P}$	0.512802(1)	0.5130
$2^3\mathrm{S} \rightarrow 4^3\mathrm{P}$	0.057527(2)	0.05754	$3^3\mathrm{S} \rightarrow 4^3\mathrm{P}$	0.186859(2)	0.18683
$2^3\mathrm{S} \rightarrow 5^3\mathrm{P}$	0.025591(2)	0.02560	$3^3\mathrm{S} \rightarrow 5^3\mathrm{P}$	0.061424(2)	0.06142
$2^3\mathrm{S} \rightarrow 6^3\mathrm{P}$	0.013742(2)	0.013745	$3^3\mathrm{S} \rightarrow 6^3\mathrm{P}$	0.028725(2)	0.028719
$2^3\mathrm{S} \rightarrow 7^3\mathrm{P}$	0.008275(3)		$3^3\mathrm{S} \rightarrow 7^3\mathrm{P}$	0.016041(2)	
$2^3\mathrm{S} \rightarrow 8^3\mathrm{P}$	0.005384(3)		$3^3\mathrm{S} \rightarrow 8^3\mathrm{P}$	0.009969(2)	
$2^3\mathrm{S} \rightarrow 9^3\mathrm{P}$	0.003707(4)		$3^3\mathrm{S} \rightarrow 9^3\mathrm{P}$	0.006658(3)	
$2^3\mathrm{S} \rightarrow 10^3\mathrm{P}$	0.002666(5)		$3^3\mathrm{S} \rightarrow 10^3\mathrm{P}$	0.004689(5)	
$2^3\mathrm{P} \rightarrow 3^3\mathrm{D}$	0.624654(1)	0.624659	$3^3\mathrm{P} \rightarrow 3^3\mathrm{D}$	0.090760(1)	0.0908
$2^3\mathrm{P} \rightarrow 4^3\mathrm{D}$	0.123214(1)	0.123214	$3^3\mathrm{P} \rightarrow 4^3\mathrm{D}$	0.503386(2)	0.50338
$2^3\mathrm{P} \rightarrow 5^3\mathrm{D}$	0.046797(2)	0.046795	$3^3\mathrm{P} \rightarrow 5^3\mathrm{D}$	0.127843(2)	0.12785
$2^3\mathrm{P} \rightarrow 6^3\mathrm{D}$	0.023278(2)	0.023277	$3^3\mathrm{P} \rightarrow 6^3\mathrm{D}$	0.053872(2)	0.05388
$2^3\mathrm{P} \rightarrow 7^3\mathrm{D}$	0.013426(2)		$3^3\mathrm{P} \rightarrow 7^3\mathrm{D}$	0.028472(3)	
$2^3\mathrm{P} \rightarrow 8^3\mathrm{D}$	0.008505(2)		$3^3\mathrm{P} \rightarrow 8^3\mathrm{D}$	0.017118(3)	
$2^3\mathrm{P} \rightarrow 9^3\mathrm{D}$	0.005752(5)		$3^3\mathrm{P} \rightarrow 9^3\mathrm{D}$	0.011189(4)	
$2^3\mathrm{P} \rightarrow 10^3\mathrm{D}$	0.00409(2)		$3^3\mathrm{P} \rightarrow 10^3\mathrm{D}$	0.00777(2)	
$2^3\mathrm{P} \rightarrow 2^3\mathrm{P}^\mathrm{e}$	0.22254(2)		$3^3\mathrm{P} \rightarrow 3^3\mathrm{P}^\mathrm{e}$	0.14741(2)	
$2^3\mathrm{P} \rightarrow 4^3\mathrm{S}$	0.007158(1)		$3^3\mathrm{P} \rightarrow 4^3\mathrm{S}$	0.084995(1)	
$2^3\mathrm{P} \rightarrow 5^3\mathrm{S}$	0.002688(1)		$3^3\mathrm{P} \rightarrow 5^3\mathrm{S}$	0.015993(1)	
$2^3\mathrm{P} \rightarrow 6^3\mathrm{S}$	0.001330(1)		$3^3\mathrm{P} \rightarrow 6^3\mathrm{S}$	0.006149(1)	
$2^3\mathrm{P} \rightarrow 7^3\mathrm{S}$	0.000765(1)		$3^3\mathrm{P} \rightarrow 7^3\mathrm{S}$	0.003112(1)	
$2^3\mathrm{P} \rightarrow 8^3\mathrm{S}$	0.000483(1)		$3^3\mathrm{P} \rightarrow 8^3\mathrm{S}$	0.001825(1)	
$2^3\mathrm{P} \rightarrow 9^3\mathrm{S}$	0.000326(1)		$3^3\mathrm{P} \rightarrow 9^3\mathrm{S}$	0.001174(1)	
$2^3\mathrm{P} \rightarrow 10^3\mathrm{S}$	0.000231(2)		$3^3P \rightarrow 10^3S$	0.000805(1)	

2.3. Dynaimc dipole polarizabilities

When an atom or ion is exposed at the external electric field with the photon energy of ω, the dynamic dipole polarizabilities for the magnetic sub-level $|N_g L_g M_g\rangle$ with the main quantum number N_g, angular momentum quantum number L_g, and magnetic quantum number M_g, can be expressed as

$$\alpha_{L_g M_g}(\omega) = \alpha_1^{\mathrm{S}}(\omega) + \frac{3M_g^2 - L_g(L_g+1)}{L_g(2L_g-1)}\alpha_1^{\mathrm{T}}(\omega), \qquad (5)$$

where $\alpha_1^{\mathrm{S}}(\omega)$ and $\alpha_1^{\mathrm{T}}(\omega)$ are the dynamic scalar and tensor dipole polarizabilities, respectively, they can be written as the summation of all the intermediate states including the continuum[39]

$$\alpha_1^{\mathrm{S}}(\omega) = \sum_{n\neq g} \frac{f_{gn}^{(1)}}{(\Delta E_{gn})^2 - \omega^2}, \qquad (6)$$

$$\alpha_1^{\mathrm{T}}(\omega) = \sum_{n\neq g} (-1)^{L_g+L_n} \sqrt{\frac{30(2L_g+1)L_g(2L_g-1)}{(2L_g+3)(L_g+1)}} \times \begin{Bmatrix} 1 & 1 & 2 \\ L_g & L_g & L_n \end{Bmatrix} \frac{f_{gn}^{(1)}}{(\Delta E_{gn})^2 - \omega^2}. \qquad (7)$$

Using the energies and oscillator strengths of the Li^+ ion, the dynamic dipole polarizabilities can be calculated. Table 3 presents a convergence test of the static dipole polarizability for the 2^3S state of the Li^+ ion. It is seen clearly that under

the same number of partial wave $\ell_{\max}$, the static dipole polarizability is decreased as the number of B-spline N increased, while the result is increased as $\ell_{\max}$ increased under the same N. This kind of convergence style for the Li^+ ion is similar to our previous work of the static dipole polarizabilities for helium.[39] Combining the different convergent trends of the static dipole polarizability as N and $\ell_{\max}$, an extrapolated value of 46.87980(1) a_0^3 is given in the last line of Table 3, which is in good agreement with the Hylleraas value of 46.8798023(7) a_0^3.[36] Comparing our extrapolated result with the variation-perturbation result of 46.8798 a_0^3 of Chen,[34] the first five digits are the same. For other triplet 2^3P, 3^3S, and 3^3P states, the final extrapolated values of static dipole polarizabilities are listed in the first line of the Table 4. The present result of the scalar static dipole polarizability for the 2^3P state agrees with the Hylleraas value of −5.790965718(2) a_0^3 (Refs. [35] and [36]) at the level of about 3-ppm accuracy.

Table 3. Convergence of the static dipole polarizabilities (in unit a.u.) for the 2^3S state of the Li^+ ion as the number of B-spline N and partial waves $\ell_{\max}$ increased. The number in parenthesis for the extrapolated value gives the computational uncertainty.

$\ell_{\max}$	$N = 30$	$N = 35$	$N = 40$
2	46.843384319	46.843377728	46.843375925
3	46.874079650	46.874071638	46.874069340
4	46.878378877	46.878369938	46.878367256
5	46.879340066	46.879330584	46.879327626
6	46.879626709	46.879616945	46.879613803
7	46.879730695	46.879720802	46.879717530
8	46.879774166	46.879764216	46.879760888
9	46.879794392	46.879784446	46.879781074
10	46.879804620	46.879794696	46.879791293
Extrap.		46.87980(1)	

Table 4. Dynamic dipole polarizabilities (in unit a.u.) of the 2^3S, 2^3P, 3^3S, and 3^3P states for the Li^+ ion. The numbers in parentheses represent computational uncertainties.

	2^3S		3^3S	2^3P		3^3P	
ω	$\alpha_1^S(\omega)$	Ref. [37]	$\alpha_1^S(\omega)$	$\alpha_1^S(\omega)$	$\alpha_1^T(\omega)$	$\alpha_1^S(\omega)$	$\alpha_1^T(\omega)$
0.000	46.87980(1)	46.961(93)	1113.569 5(5)	−5.79095(2)	13.4416(2)	1144.39(2)	205.118(2)
0.005	47.04279(2)	47.125(94)	1175.622 7(6)	−5.84300(3)	13.495 5(2)	2074.52(2)	130.689(2)
0.010	47.53897(2)	47.622(95)	1412.449(2)	−6.00155(3)	13.659 5(2)	−2845.15(3)	693.603(3)
0.015	48.39072(2)	48.478(97)	2132.891(3)	−6.27402(3)	13.9409(3)	−1196.29(3)	744.677(4)
0.020	49.63818(3)	49.726(100)	7637.82(6)	−6.67378(3)	14.353 5(2)	−2739.42(2)	2550.22(2)
0.025	51.34429(2)	51.436(104)	−3234.71(2)	−7.22175(3)	14.917 8(2)	994.02(3)	−1085.2(1)
0.030	53.60333(3)	53.700(100)	−1168.05(1)	−7.94928(3)	15.6655(2)	360.07(3)	−402.25(2)
0.035	56.55543(3)	56.659(117)	−659.409(1)	−8.90302(3)	16.6432(3)	223.211(2)	−236.51(2)
0.040	60.4118(1)	60.524(127)	−434.945(1)	−10.153(1)	17.921(1)	170.379(2)	−164.57(2)
0.045	65.500 1(1)	65.624(140)	−310.938(1)	−11.809(2)	19.609(2)	145.459(2)	−125.73(2)
0.050	72.351 6(1)	72.490(157)	−233.427(1)	−14.048(2)	21.883(2)	133.125(3)	−102.32(3)
0.055	81.881 6(1)	82.042(182)	−180.951(1)	−17.174(2)	25.049(1)	127.833(2)	−87.424(2)
0.060	95.805 8(1)	95.997(218)	−143.323(1)	−21.759(2)	29.679(2)	127.353(2)	−77.886(2)
0.065	117.750(1)	117.991(275)	−115.105(1)	−29.012(3)	36.981(2)	130.950(2)	−72.205(2)
0.070	156.919(1)	157.247(378)	−93.126 7(1)	−42.000(2)	50.023(4)	138.858(3)	−69.832(2)
0.075	245.507(1)	246.025(617)	−75.4013(1)	−71.455(2)	79.537(1)	152.422(2)	−71.086(1)
0.080	629.50(1)	630.78(174)	−60.5973(1)	−199.37(2)	207.519(2)	175.141(2)	−77.849(2)
0.085	−919.55(2)	−914.94(916)	−47.7456(1)	317.066(2)	−308.853(2)	217.321(2)	−97.391(3)
0.090	−252.407(2)	−252.45(128)	−36.0554(1)	94.776(3)	−86.489(2)	336.962(3)	−180.864(2)
0.11	−56.776 0(2)	−56.89(26)	20.7214(1)	30.021(2)	−21.374(2)	−493.223(2)	56.597(2)
0.13	−28.360 1(2)	−28.43(16)	−138.670(1)	21.155(2)	−12.029(3)	−54.399 5(2)	1.1613(4)
0.15	−17.23964(4)	−17.30(13)	−36.150(2)	18.255(2)	−8.494 1(2)	1088.04(4)	−102.66(4)
0.17	−11.39972(2)	−11.45(12)	559.55(3)	17.397(3)	−6.780 6(2)	5.4805(4)	−12.4600(4)
0.19	−7.821 74(2)	−7.87(12)	−14.789(4)	17.716(3)	−5.917 5(2)	−223.59(4)	24.67(5)
0.21	−5.39206(2)	−5.45(12)	38.53(3)	19.105(4)	−5.603 7(3)		
0.23	−3.600 13(1)	−3.66(13)	−20.52(4)	21.970(5)	−5.843 4(4)		
0.25	−2.17019(1)	−2.25(16)		27.830(5)	−7.1771(5)		
0.27	−0.924 47(1)	−1.03(20)		48.032(6)	−17.758(4)		
0.29	0.28651(1)	0.13(27)		68.856(6)	−3.9146(4)		
0.31	1.650 22(2)	1.39(43)		−208.2(3)	21.345(2)		
0.33	3.542 89(1)	3.02(78)		−35.52(4)	3.4899(2)		
0.35	7.218 69(1)	5.87(185)		−15.87(4)	1.2419(2)		
0.37	23.45933(4)	16.23(909)		−6.489(4)	0.0019(3)		
0.38	918.6(2)	505(495)		−1.685(5)	−0.8921(3)		

The dynamic dipole polarizabilities for the 2^3S state of the Li^+ ion for some selective photon energy of $0 \leq \omega \leq 0.38$ a.u. are listed in Table 4. The figures in parentheses represent computational uncertainties. It can be seen that all of the present values have at least four significant figures except the result of 918.6(2) a_0^3 for $\omega = 0.38$ a.u., where the photon energy lies near the second resonance excitation threshold of 0.38031 a.u. Comparing our results with the values of Glover and Weinhold,[37] all of our values lie within the upper and lower limits of their values. In addition, Table 4 also lists the dynamic dipole polarizabilities for the 2^3P, 3^3S, and 3^3P states. For the 3^3S state, present values have 5–7 significant digits with $\omega \leq 0.13$ a.u. For the 2^3P and 3^3P states, all of the results for the scalar and tensor dipole polarizabilites have at least four significant digits except values for the photon energy ω near the resonance transition position or ionization threshold.

2.4. Tune-out and magic wavelengths

The tune-out wavelength is defined as the wavelength which makes the dynamic dipole polarizability of a single state disappear.[49,50] The magic wavelength is defined as the wavelength which makes the dynamic dipole polarizabilities of the upper and lower energy levels of a transition equal.[51–53] The dynamic dipole polarizabilities for the lowest four triplet states of the Li^+ ion are also plotted in Figs. 2–7 as the photon energy ω increased. The crossing points between a curve and the horizontal zero line are labeled as tune-out wavelengths, which denoted as a solid magenta circle. The crossing points between two curves are the magic wavelengths, which are denoted as a blank red circle. The vertical dashed lines are the resonance transition positions.

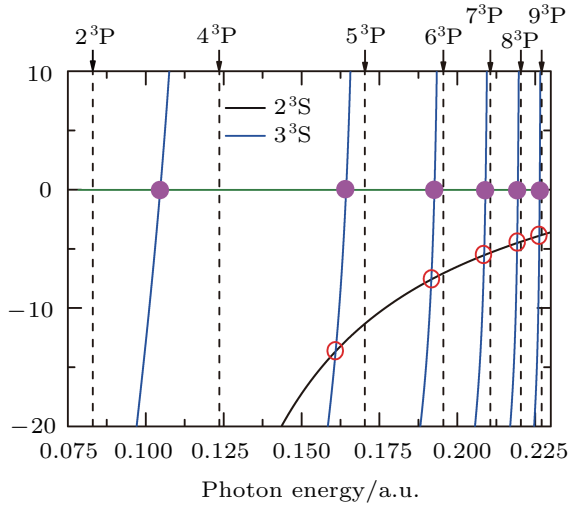


Fig. 2. (color online) Dynamic dipole polarizabilities (in unit a.u.) of the Li^+ ion for the photon energy $0.075 \leq \omega \leq 0.225$ a.u. The solid black line denotes the dynamic polarizabilities for the 2^3S state, and the solid blue line represents the dynamic polarizabilities for the 3^3S state. The crossing points denoted as solid magenta circles are the tune-out wavelengths, and the crossing points denoted as blank red circles are the magic wavelengths. The vertical dashed lines are the resonance transition positions, and the green line is a horizonal zero line.

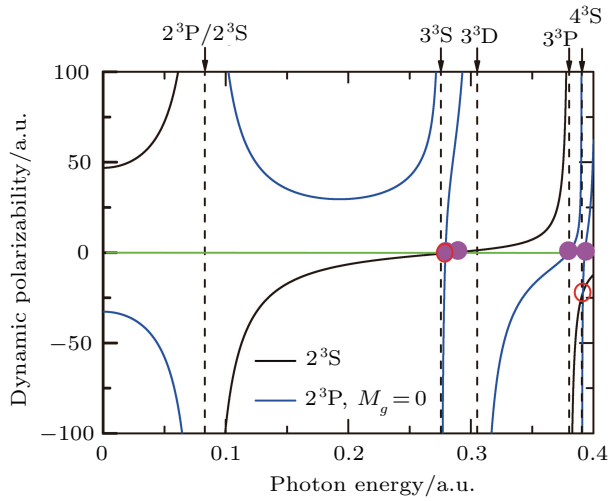


Fig. 3. (color online) Dynamic dipole polarizabilities (in unit a.u.) of the Li^+ ion for the photon energy $0.0 \leq \omega \leq 0.40$ a.u. The solid black line denotes the dynamic polarizabilities for the 2^3S state, and the solid blue line represents the dynamic polarizabilities for the 2^3P ($M_g = 0$) state.

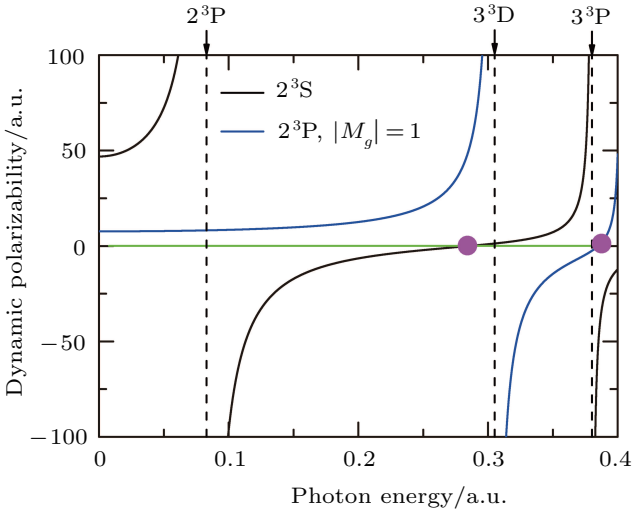


Fig. 4. (color online) Dynamic dipole polarizabilities (in unit a.u.) of the Li^+ ion for the photon energy $0.0 \leq \omega \leq 0.4$ a.u. The solid black line denotes the dynamic polarizabilities for the 2^3S state, and the solid blue line represents the dynamic polarizabilities for the 2^3P ($|M_g| = 1$) state.

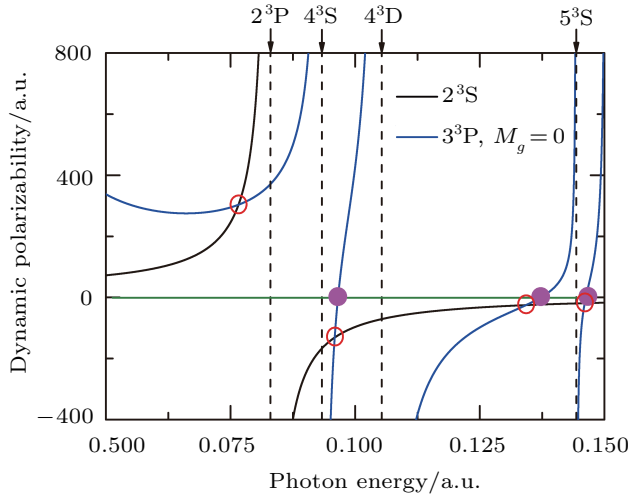


Fig. 5. (color online) Dynamic dipole polarizabilities (in unit a.u.) of the Li^+ ion for the photon energy $0.050 \leq \omega \leq 0.150$ a.u. The solid black line denotes the dynamic polarizabilities for the 2^3S state, and the solid blue line represents the dynamic polarizabilities for the 3^3P ($M_g = 0$) state.

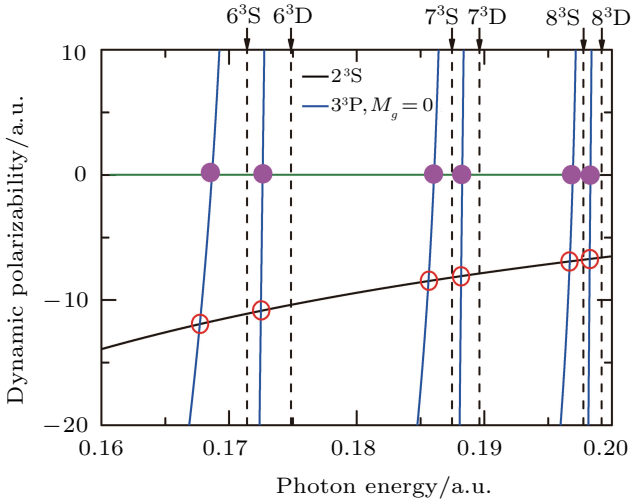


Fig. 6. (color online) Dynamic dipole polarizabilities (in unit a.u.) of the Li^+ ion for the photon energy $0.16 \leq \omega \leq 0.20$ a.u. The solid black line denotes the dynamic polarizabilities for the 2^3S state, and the solid blue line represents the dynamic polarizabilities for the 3^3P ($M_g = 0$) state.

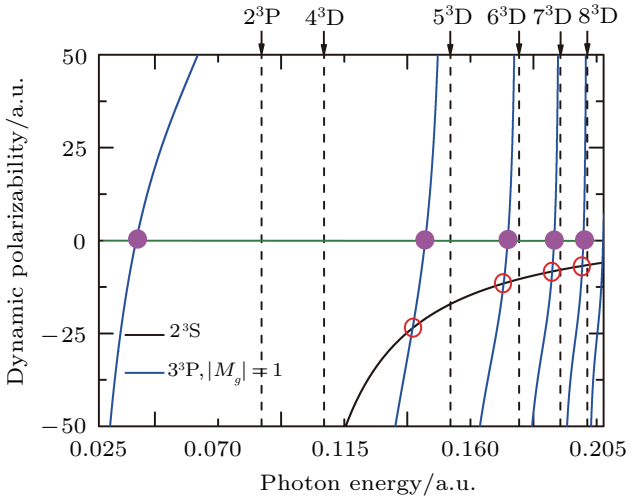


Fig. 7. (color online) Dynamic dipole polarizabilities (in unit a.u.) of the Li^+ ion for the photon energy $0.025 \leq \omega \leq 0.205$ a.u. The solid black line denotes the dynamic polarizabilities for the 2^3S state, and the solid blue line represents the dynamic polarizabilities for the 3^3P ($|M_g| = 1$) state.

Table 5. Tune-out wavelengths λ_t (in unit nm) for 2^3S, 3^3S, 2^3P, and 3^3P states of the Li^+ ion. The numbers in parentheses give the computational uncertainties.

2^3S	3^3S	2^3P		3^3P	
		$M_g = 0$	$\|M_g\| = 1$	$M_g = 0$	$\|M_g\| = 1$
159.672(1)	435.38(1)	163.141(2)	118.354(1)	471.86(1)	1190.14(3)
	277.288(2)	119.940(1)		331.940(3)	322.267(5)
	236.500(1)	115.941(1)		311.485(2)	266.78(1)
	217.972(2)			270.143(3)	243.197(6)
	207.651(2)			263.936(2)	230.372(2)
	201.213(2)			244.880(1)	
				242.008(1)	
				231.361(6)	
				229.749(1)	

Table 6. Magic wavelengths λ_m (in unit nm) for $2^3S \rightarrow 3^3S$, $2^3S \rightarrow 2^3P$, and $2^3S \rightarrow 3^3P$ transitions of the Li^+ ion. The numbers in parentheses give the computational uncertainties.

$2^3S \rightarrow 3^3S$	$2^3S \rightarrow 2^3P$ ($M_g = 0$)	$2^3S \rightarrow 3^3P$ ($M_g = 0$)	$2^3S \rightarrow 3^3P$ ($\|M_g\| = 1$)
283.108(2)	163.156(1)	594.78(1)	332.866(5)
237.738(2)	116.387(1)	475.12(1)	269.050(3)
218.419(2)		339.346(5)	244.089(3)
207.857(2)		311.971(4)	230.821(4)
201.324(2)		271.678(5)	
		264.146(3)	
		245.456(3)	
		242.120(3)	
		231.641(3)	
		229.816(4)	

The values of the tune-out and magic wavelengths in the Figs. 2–7 are listed in Tables 5 and 6, respectively. It is noticed that most tune-out wavelengths are in the range of 110 nm–500 nm except for the tune-out wavelength of 1190.14(3) nm for the 3^3P ($|M_g| = 1$) state. All the values of magic wavelengths are in the range of 110 nm–600 nm. All the tune-out wavelengths in Table 5 have at least four significant digits, and all the present magic wavelengths in Table 6 have five significant digits. These accurate theoretical values of tune-out and magic wavelengths can be used as important parameters for experiment design to trap the Li^+ ion for high-precision measurements.

3. Conclusions

The *ab-initio* calculations of the dynamic dipole polarizabilities for the four lowest triplet states (2^3S, 3^3S, 2^3P, and 3^3P) of the Li^+ ion are carried out by using the B-spline CI method. The large number of accurate energies and oscillator strengths with the main quantum number n up to 10 of the Li^+ ion are tabulated for theoretical references. Present static dipole polarizabilities for the 2^3S and 2^3P states are in excellent agreement with the most accurate results from variational Hylleraas basis calculations,[35,36] and present dynamic dipole polarizabilities for the 2^3S state that lies within the upper and lower bounds of the values from the correlated variational trial function calculation.[37] In addition, the tune-out wavelengths for the four lowest triplet states, and the magic wavelengths for the three transitions of $2^3\text{S} \rightarrow 3^3\text{S}$, $2^3\text{S} \rightarrow 2^3\text{P}$, and $2^3\text{S} \rightarrow 3^3\text{P}$ are identified with at least four significant digits. Present polarizabilities provide theoretical references for analyzing the Stark shift of the Li^+ ion. Our tune-out and magic wavelengths can be used for designing the high-precision experimental measurement on the Li^+ ion in the future.

References

[1] Kowalski J, Neumann R, Noehte S, Scheffzek K, Suhr H and Putlitz G Z 1983 *Hyp. Int.* **15** 159
[2] Clarke J J and van Wijngaarden W A 2003 *Phys. Rev. A* **67** 012506
[3] Riis E, Sinclair A G, Poulsen O, Drake G W F, Rowley W R C and Levick A P 1994 *Phys. Rev. A* **49** 207
[4] Pachucki K and Yerokhin V A 2009 *Phys. Rev. A* **79** 062516
[5] Zelevinsky T, Farkas D and Gabrielse G 2005 *Phys. Rev. Lett.* **95** 203001
[6] Borbely J S, George M C, Lombardi L D, Weel M, Fitzakerley D W and Hessels E A 2009 *Phys. Rev. A* **79** 060503
[7] Pachucki K and Yerokhin V A 2010 *Phys. Rev. Lett.* **104** 070403
[8] Zhang P P, Zhong Z X, Yan Z C and Shi T Y 2015 *Chin. Phys. B* **24** 033101
[9] Rong H, Grafström S, Kowalski J, Putlitz G z, Jastrzebski W and Neumann R 1993 *Z. Phys. D* **25** 337
[10] Wijngaarden W A van and Noble G A 2008 *Lect. Notes Phys.* **745** 111
[11] Botermann B, Bing D, Geppert C, Gwinner G, Hänsch T W, Huber G, Karpuk S, Krieger A, Kühl T, Nörtershäuser W, Novotny C, Reinhardt S, Sánchez R, Schwalm D, Stöhlker T, Wolf A and Saathoff G 2014 *Phys. Rev. Lett.* **113** 120405
[12] Arora B and Sahoo B K 2014 *Phys. Rev. A* **89** 022511
[13] Porsev S G, Safronova M S, Derevianko A and Clark C W 2014 *Phys. Rev. A* **89** 022703
[14] Mitroy J, Safronova M S and Clark C W 2010 *J. Phys. B: At. Mol. Opt. Phys.* **43** 202001
[15] Ward S J and Shertzer J 2004 *Nucl. Instrum. Method Phys. Res. B* **221** 206
[16] Han H, Zhong Z, Zhang X and Shi T 2008 *Phys. Rev. A* **78** 044701
[17] Liu P L, Huang Y, Bian W, Shao H, Guan H, Tang Y B, Li C B, Mitroy J and Gao K L 2015 *Phys. Rev. Lett.* **114** 223001
[18] Tang L Y, Bromley M W J, Yan Z C and Mitroy J 2013 *Phys. Rev. A* **87** 032507
[19] Farley J W and Wing W H 1981 *Phys. Rev. A* **23** 2397
[20] Safronova M S, Safronova U I and Clark C W 2012 *Phys. Rev. A* **86** 042505
[21] Yu W W, Yu R M, Cheng Y J and Zhou Y J 2016 *Chin. Phys. B* **25** 023101
[22] Udem Th, Holzwarth R and Hänsch T W 2002 *Nature* **416** 233
[23] Margolis H S 2009 *J. Phys. B: At. Mol. Opt. Phys.* **42** 154017
[24] Bloom B J, Nicholson T L, Williams J R, Campbell S L, Bishof M, Zhang X, Zhang W, Bromley S L and Ye J 2014 *Nature* **506** 71
[25] Glover R M and Weinhold F 1976 *J. Chem. Phys.* **65** 4913
[26] Bishop D M and Rérat M 1989 *J. Chem. Phys.* **91** 5489
[27] Banerjee A and Harbola M K 1997 *Pramana J. Phys.* **49** 455
[28] Bhatia A K and Drachman R J 1997 *Can. J. Phys.* **75** 11
[29] Zhu J M, Zhou B L and Yan Z C 1999 *Chem. Phys. Lett.* **313** 184
[30] Johnson W R and Cheng K T 1996 *Phys. Rev. A* **53** 1375
[31] Bhatia A K and Drachman R J 1997 *Phys. Rev. A* **55** 1842
[32] Lim I S, Laerdahl J K and Schwerdtfeger P 2002 *J. Chem. Phys.* **116** 172
[33] Chung K T 1971 *Phys. Rev. A* **4** 7
[34] Chen M K 1995 *J. Phys. B: At. Mol. Opt. Phys.* **28** 1349
[35] Zhu J M, Zhou B L and Yan Z C 2000 *Mol. Phys.* **98** 529
[36] Yan Z C, Zhu J M and Zhou B L 2000 *Phys. Rev. A* **62** 034501
[37] Glover R M and Weinhold F 1977 *J. Chem. Phys.* **66** 185
[38] Glover R M and Weinhold F 1977 *J. Chem. Phys.* **66** 191
[39] Zhang Y H, Tang L Y, Zhang X Z and Shi T Y 2015 *Phys. Rev. A* **92** 012515
[40] Lin Y C, Fang T K and Ho Y K 2015 *Phys. Plasmas* **22** 032113
[41] Yulian V V and Alejandro S 2004 *J. Phys. B: At. Mol. Opt. Phys.* **37** 4101
[42] Nikolopoulos L A A 2003 *Comput. Phys. Commun.* **150** 140
[43] Kramida A, Ralchenko Y, Reader J and NIST ASD Team 2012 "NIST Atomic Spectra Database" (version 5.0.0), URL http://physics.nist.gov/asd
[44] Cann N M and Thakkar A J 1992 *Phys. Rev. A* **46** 5397
[45] Accad Y, Pekeris C L and Schiff B 1971 *Phys. Rev. A* **4** 516
[46] Godefroid M and Verhaegen G 1980 *J. Phys. B: At. Mol. Opt. Phys.* **13** 3081
[47] Schiff B, Pekeris C L and Accad Y 1971 *Phys. Rev. A* **4** 885
[48] Kono A and Hattori S 1984 *Phys. Rev. A* **30** 2093
[49] LeBlanc L J and Thywissen J H 2007 *Phys. Rev. A* **75** 053612
[50] Mitroy J and Tang L Y 2013 *Phys. Rev. A* **88** 052515
[51] Ye J, Vernooy D W and Kimble H J 1999 *Phys. Rev. Lett.* **83** 4987
[52] Katori H, Ido T and Kuwata-Gonokami M 1999 *J. Phys. Soc. Jpn.* **68** 2479
[53] Safronova M S, Safronova U I and Clark C W 2013 *Phys. Rev. A* **87** 052504